

---

## Effect of temperature and CO<sub>2</sub> concentration on the morphogenesis of sagittal otoliths in Atlantic herring (*Clupea harengus*) larvae

Mahé Kélig <sup>1,\*</sup>, Joly Léa <sup>1,2</sup>, Telliez Solène <sup>1</sup>, Zambonino Infante José-Luis <sup>2</sup>, Meunier Cédric Léo <sup>3</sup>, Mackenzie Kirsteen <sup>1</sup>, Giraldo Carolina <sup>1</sup>

<sup>1</sup> Ifremer, Fisheries laboratory, Channel and North Sea Fisheries Research Unit, Boulogne-sur-mer, France

<sup>2</sup> Ifremer, Univ Brest, CNRS, IRD, LEMAR, Plouzané, France

<sup>3</sup> Helmholtz-Zentrum für Polar- und Meeresforschung, Alfred-Wegener-Institut, Helgoland, Germany

\* Corresponding author : Kélig Mahé, email address : [kelig.mahe@ifremer.fr](mailto:kelig.mahe@ifremer.fr)

---

### Abstract :

Otoliths are very useful biomarkers especially for fish growth. Climate change with the associated global changes in warming and acidification could affect the calcification and the shape of otoliths during the crucial larval period in teleost fish. To evaluate this predicted combined effect of temperature and CO<sub>2</sub>, Atlantic herring (*Clupea harengus*) embryos and larvae were reared from hatching to respectively 47 and 60 days post-hatching (dph), under present day conditions and a scenario predicted for the year 2100 (IPCC RCP8.5). Otolith morphogenesis was tracked by analyzing area and normalized Elliptical Fourier coefficients. We found that otolith area for fish of similar size increased under the predicted 2100 climate change scenario compared to the present day. Climate change does not, however, seem to directly affect the otolith shape. Finally, the onset of otolith morphogenesis is hardwired, but the relationship between otolith and fish size is environment-dependent.

### Highlights

► Climate change do not affect the otolith shape of the herring larvae ► No directional bilateral asymmetry found between left and right otoliths ► Relationship between otolith and fish size is environment-dependent

**Keywords :** Otolith shape, Otolith area, Temperature effect, Ocean acidification, Elliptic Fourier descriptors, Directional asymmetry

## 25 ***1. Introduction***

26 Otoliths are calcified biomineralised structures overlying the sensory epithelia in the inner ear of fish.  
27 They are formed by calcium carbonate crystals embedded in a non-collagenous organic matrix  
28 composed of acidic proteins and polysaccharides (Degens et al., 1969; Popper et al., 2005). They are  
29 metabolically inert and do not resorb in periods of stress, but grow throughout an individual's life, in  
30 correlation with its ontogenic growth (Casselman, 1987). Because of the positive correlation  
31 between otolith and fish growths, otoliths have been widely used in fisheries science to understand  
32 the fish growth and the potential effects which controlled it (i.e. environment, fishing pressure;  
33 Enberg et al., 2011 ; Marty et al., 2014; Carbonara et al., 2022). In Atlantic herring (*Clupea*  
34 *harengus*), otolith microstructure has been used to study environmental effects (temperature, salinity  
35 or feeding activity) on the growth of the larvae (Folkvord et al., 1997 ; 2004 ; Johannessen et al.,  
36 2000; Berg et al., 2017; Denis et al., 2017; Tonheim et al., 2020), and otolith shape used as a tool for  
37 stock identification (Turan, 2000; Burke et al., 2008; Libungan et al., 2015). Atlantic herring are of  
38 high commercial importance, with around 1,640,000 tons caught in 2016 (FAO FishStat data), but  
39 are vulnerable to the effects of climate change, particularly at the larval stage (Hufnagl and Peck,  
40 2011).

41 Otolith growth, and ultimately global otolith shape are well-known to result from the combination of  
42 genetic heterogeneity, ontogeny (physiological processes) and the influence of environmental (biotic  
43 and abiotic) factors (Vignon and Morat, 2010; Mahé, 2019; Hüsey et al., 2020). Global climate  
44 change is projected to cause warming of the ocean surface by 3 to 5°C by 2100, and acidification of  
45 waters with a drop of 0.4 pH units in the worst-case scenario (IPCC 2019). The speed at which global  
46 change is occurring will not allow some species to adapt; in addition, early life history stages which  
47 do not yet have fully functional physiological homeostatic mechanisms could be particularly affected

48 (Melzner et al., 2009). Some ontogenic processes, such as otolith morphogenesis, could thus be  
49 particularly impacted by the alteration of environmental conditions.

50 A previous study on herring larvae testing four temperature conditions showed that the size and the  
51 width of the otolith daily increment were both temperature-dependent (Folkvord et al., 2004). Other  
52 studies on the effects of ocean acidification on fish otoliths have been mostly conducted on larval  
53 developmental stages. Several studies have shown that elevated levels of CO<sub>2</sub> caused an increase in  
54 otolith size or modification of the otolith shape for multiple species (Munday et al., 2011; Bignami et  
55 al., 2013; Maneja et al., 2013; Reveillac et al., 2015; Coll-Llado et al., 2021). Consequently,  
56 acidification can lead to decoupling of otolith and body growth for some species (Reveillac et al.,  
57 2015; Franke and Clemmesen 2011; Frommel et al., 2013; Perry et al., 2021).

58 Here, we aimed to investigate in Atlantic herring how otolith shape and size variability is affected by  
59 the warming and acidification conditions projected by 2100 under the worst-case IPCC scenario  
60 during the first early life stages. This otolith shape was investigated within individual (i.e. directional  
61 bilateral asymmetry) and within the population (i.e. between individuals).

62

## 63 ***2. Materials and methods***

### 64 **2.1 Experimental design**

65 A experiment with temperature and CO<sub>2</sub> concentration (through the measure of pCO<sub>2</sub> as partial  
66 pressure of CO<sub>2</sub>) as combined factors was conducted, one close to present day conditions of  
67 temperature and pH in the winter in the English Channel (Amb; 11°C and pH 8.0, pCO<sub>2</sub> ~560 µatm),  
68 and the other a global change scenario of ocean warming and acidification (IPCC 2019, “Changing  
69 ocean, marine ecosystems and dependent communities”) (OWA; 14°C and pH 7.6, pCO<sub>2</sub> ~1660  
70 µatm) (Supplementary Table 1). There were 3 replicates (tanks) for each experimental condition (i.e.

71 temperature-CO<sub>2</sub>). Most of the eggs hatched on the 9th day of incubation (starting point of the  
72 experiment: 1 dph) and larvae were kept until 69 days post hatch (dph). Three days after hatching (3  
73 dph), all larvae were counted and distributed equally in six 38 L conical black tanks (1500 larvae by  
74 tank), constituting the replicates of the experiment. A continuous flow through system of 20 L h<sup>-1</sup>  
75 was used (i.e. open circulation system). To allow the acclimation of the larvae, the temperature in the  
76 OWA tanks was progressively increased from 11 to 14°C over 48 h. Each OWA tank was supplied  
77 by a 200 L header tank, where the heated water was enriched with CO<sub>2</sub> to achieve the target value of  
78 pH 7.6.

79 Temperature and CO<sub>2</sub> were checked twice per day (pH meter 330i, WTW, Germany; Table S1).  
80 Oxygen saturation (oximeter: WTW Oxi 340, Bioblock scientific) and salinity were measured once  
81 per week, along with total alkalinity (TA) of each tank following the protocol of Anderson and  
82 Robinson (1946) and Strickland and Parsons (1972). Oxygen concentration was always above 88%.  
83 pCO<sub>2</sub> was calculated using the excel macro CO<sub>2</sub>sys (Lewis and Wallace 1998) with the constant  
84 from Mehrbach et al., (1973) refit by Dickson and Millero (1987). To prevent any food limitation, the  
85 daily food quantity was distributed four times during the day to maintain an ad libitum level (Strain  
86 2002), ensuring that there were always prey in the tank during the day. To be sure to allow proper  
87 feeding through time we used an increasing range of living prey sizes from phytoplankton to 24 h old  
88 nauplii, before weaning with feed granules (as described in Joly et al., 2021). Throughout the study,  
89 mortality was monitored daily, and was comparable between all ponds with no influence of  
90 environmental conditions (for more details, Joly et al., 2021).

91 Experimental animal came from wild Atlantic herring from the Downs stock of the southern North  
92 Sea and English Channel (Joly et al., 2021). Herring larvae were reared until they reached the last  
93 larval development stage respectively from hatching to 47 days post-hatching in the OWA treatment  
94 (14°C, 1660 µatm) and 60 days post-hatching in the Amb treatment (11°C, 560 µatm) to obtain the

95 same Growing Degree Days (GDD) for two temperature conditions. To follow the otolith growth and  
96 shape variation through time, 351 Atlantic herring from 32 to ~662°C.day (GDD, Figure 1) were  
97 sampled five times over the course of the experiment. At 32°C.day, 15 individuals were sampled, and  
98 then 42 fish for each experimental condition were sampled at each of the next four samplings. To  
99 assess the potential effect of temperature on the growth and shape of otoliths, we used the GDD  
100 approach which quantifies the thermal opportunity for growth by aggregating temperatures relevant  
101 to growth (McMaster and Wilhelm, 1997), and is thus more precise than the calendar time approach  
102 when describing growth (Neuheimer and Taggart, 2007; Mahé et al., 2019). The first sampling  
103 occurred at three days post-hatching (GDD=32°C.day). The four other samplings were then carried  
104 out after different time periods depending on the rearing temperature (Figure 1).

## 105 **2.2 Otolith shape analysis**

106 After measuring the total length ( $TL \pm 0.1$  cm) of fish, their sagittal otoliths (left and right) were  
107 extracted from the cranial cavity and cleaned. The outline of each otolith was digitized using an  
108 image analysis system. To compare the shapes of the left and right otoliths, mirror images of the right  
109 otoliths were used. Otolith shape was assessed by analyzing first the otolith area (Oarea,  $\mu\text{m}^2$ ) and  
110 Elliptic Fourier Descriptors (EFDs; e.g. Lestrel, 2008). Oarea seems to be a better univariate  
111 descriptor than longest length. For each otolith, the first 99 elliptical Fourier harmonics were  
112 extracted and normalized with respect to the first harmonic so as to be invariant to otolith size,  
113 rotation and starting point of contour description (Kuhl and Giardina, 1982). To determine the  
114 number of harmonics required to reconstruct the otolith outline, the cumulated Fourier power (F) was  
115 used. Only the first 6 harmonics were necessary to ensure reconstruction of each otolith shape with a  
116 precision of  $F=99.99\%$  (Lestrel, 2008) and were thus used for further analyses.

117 The resulting matrix containing EFDs (as columns) for each otolith (as rows) was subjected to  
118 Principal Components Analysis (PCA) (Rohlf and Archie, 1984). and the 3 first principal

119 components (PCs) were selected as otolith shape descriptors or shape matrix according to the broken  
120 stick model (Legendre and Legendre, 1998), which, in this case, corresponded to a threshold of 3.4%  
121 of the total variance explained (Borcard et al., 2011). In total, these 3 PCs explained 82.4% of the  
122 total variance in the EFDs. This procedure allowed us to decrease the number of variables used to  
123 describe otolith shape variability through EFDs while ensuring that the main sources of shape  
124 variation were kept, and to avoid co-linearity between shape descriptors (Rohlf and Archie, 1984).

### 125 **2.3 Statistical analyses**

126 Each environmental condition was the combination of temperature and CO<sub>2</sub> concentration values.  
127 Otolith area and larvae size differences were analysed using a post-hoc Tukey-HSD test among  
128 several values of GDD. The relationship between larval total length (TL) and otolith area (Oarea) in  
129 response to the environmental conditions (temperature and CO<sub>2</sub> concentration) was tested using  
130 Analysis of Covariance after verifying the normality of residuals. Using the Fourier harmonics to  
131 describe the otolith shape, pRDA were used to test the explanatory variables of interest (i.e., side,  
132 combination of temperature and CO<sub>2</sub> concentration, GDD value) using total length to correct for fish  
133 size. This pRDA was combined with permutation tests on the selected PC matrix and the explanatory  
134 matrix consisted. To analyse the potential anatomical differences described by the directional  
135 bilateral asymmetry between left and right otolith shape, partial redundancy analysis (pRDA) was  
136 modelled on the selected principal components (PCs) matrix using otolith side (left/right) as the  
137 potentially influential variable and the individual as the conditioned variable. To test the potential  
138 effect of climate change, the pRDA was applied with the environmental explanatory matrix  
139 (Temperature and CO<sub>2</sub> concentration). To visualise shape differences, average shapes were rebuilt  
140 based on EFDs averaged for each group of individuals. Directional asymmetry and environmental  
141 effect amplitude were then computed as the percentage of non-overlapping surface between the  
142 reconstructed otolith average shapes relative to the total area they covered after superposition for 2

143 groups left side/right side or 2 environmental conditions as used for other otolith shape studies (Mahé  
144 et al., 2018 ; Mahé et al., 2019 ; Mahé, 2019).

145 Statistical analyses were performed using the following packages in the statistical environment R:  
146 ‘Vegan’ (Oksanen et al., 2013), ‘sp’ (Bivand et al., 2013) and ‘rgeos’ (Bivand et al., 2013).

### 147 **3. Results**

#### 148 **3.1 Otolith growth**

149 There is a positive relationship between otolith and fish larvae sizes. Otolith and larvae sizes  
150 increased stepwise from 32 to 670°C.day (Figure 2). Over the course of the experiment, the ratio  
151 between the dorso-ventral and antero-posterior axis increased, leading to the loss of the initial  
152 circular shape of the otolith. Otolith morphogenesis was positively correlated with GDD. No  
153 statistical approach was applied on this ratio between the dorso-ventral and antero-posterior axis or  
154 otolith morphogenesis because it was only the difference automatically measured from the  
155 reconstructed otolith average shapes which explained the shape evolution (because it was not  
156 available (it was not possible to realize the automatic measures of individual length along the same  
157 axis due to the shape close to the circle). Herring larvae were long and thin at hatching, then  
158 progressively developed dorsal and caudal fins. Body height increased around 436°C.day, and the  
159 pelvic fins were the last fins to differentiate at around 662°C.day. Otolith area and larvae size  
160 differences were analysed among several values of GDD. Larvae size as otolith area grow during the  
161 larvae life (i.e. with GDD value; Figure 3A). Larvae size increased significantly between 32°C.day  
162 and 87°C.day, while the first changes in otolith area appeared only at 436°C.day. However, after this  
163 GDD level, otolith area (i.e. otolith 2-dimensional measure) increased faster than larval size measure  
164 (i.e. fish 1-dimensional measure). Neither larvae size nor otolith area were significantly different  
165 between the two environmental conditions (temperature/CO<sub>2</sub>) at any value of GDD, with the  
166 exception of larvae size at 436°C.day (P<0.05). The relationship between Oarea and TL was always

167 significant ( $P < 0.05$ ), but the slope was significantly higher in the OWA than in the Amb treatment  
168 (slopes difference;  $P < 0.05$ ; Figure 3B). For the same fish length, the area of otolith was bigger for the  
169 2100 scenario ( $14^{\circ}\text{C}/\text{CO}_2$  1660  $\mu\text{atm}$ ) than under present day conditions ( $11^{\circ}\text{C}/\text{CO}_2$  560  $\mu\text{atm}$ )  
170 (Figure 3B); this difference increased with fish size. Our experimental study showed that this  
171 significant correlation between otolith and fish growth was still observed in present day  
172 environmental conditions as well as for the 2100 scenario.

### 173 **3.2 Otolith shape**

174 No significant difference in shape was observed between left and right otoliths (Supplementary Table  
175 2). The average percentage of non-overlapping surface between the two sides never exceeded 1%  
176 (Figure 4). Similarly, the results showed no significant environmental effect on otolith shape in  
177 herring larvae, with the average percentage of non-overlapping surface ranging from 0.73% to 1.48%  
178 (Supplementary Table 2; Figure 4).

## 179 **4. Discussion**

180 The otolith shape is regulated by a complex combination of endogenous and exogenous factors,  
181 including both abiotic environmental parameters (such as temperature and  $\text{CO}_2$ ), and biotic  
182 parameters (such as food availability). The influence of these factors is dependent on the ontogenetic  
183 stage (i.e. the development stage of the individual). In addition, the otoliths can be different between  
184 right and left inner ears as a consequence of potential developmental lateralization (e.g. side effect).  
185 Environmental factors, especially temperature, have a greater influence than genetic differences for  
186 Atlantic cod (Cardinale et al., 2004; Hüsey, 2008; Irgens, 2018). For seabass (*Dicentrarchus labrax*),  
187 increased temperature speeds up otolith morphogenesis and modifies the developmental pattern of  
188 the otolith shape (Mahé et al., 2019). Ocean acidification can also alter otolith shape (Holmberg et  
189 al., 2019). For several species, individuals exposed to high  $\text{CO}_2$  had a larger otolith area and  
190 maximum length compared with controls; the increases were larger than could be explained by an

191 increase in CaCO<sub>3</sub> precipitation in the otoliths driven by the modification of the pH regulation in the  
192 endolymph (Checkley et al., 2009; Munday et al., 2011; Réveillac et al., 2015; Coll-Llado et al.,  
193 2018). Changes in extracellular concentrations of carbonate and bicarbonate caused by acid-base  
194 regulation in a high CO<sub>2</sub> environment could increase the precipitation of CaCO<sub>3</sub> in the otolith (Payan  
195 et al., 1998). In studies on other species including herring, high CO<sub>2</sub> had no effect on the larval  
196 sagittal otolith (Franke and Clemmesen, 2011; Munday et al., 2011; Frommel et al., 2013; Perry et  
197 al., 2015). Our experimental study showed that there is the relationship between otolith area and fish  
198 length according to the environmental conditions and validated the results observed *in situ* (Folkvord  
199 et al., 1997; Johannessen et al., 2000; Berg et al., 2017; Denis et al., 2017; Tonheim et al., 2020). A  
200 previous study on herring larvae testing four temperature conditions (4°C, 12°C and two others  
201 shifted twice with 4/8/4°C and 12/8/12°C) showed that the size and the width of the otolith daily  
202 increment were both temperature-dependent (Folkvord et al., 2004). The otolith area per fish size in  
203 our study increased with higher temperature and CO<sub>2</sub> (i.e. lower pH). It should be noted that the  
204 feeding protocol chosen for this study provides *ad-libitum* feed, in order to avoid under-feeding  
205 situations that could have interfered with the otolith study. Nevertheless, it cannot be excluded that  
206 larvae under the 2100 scenario ingest more food than control larvae, which could also accelerate the  
207 increase of the otolith area in the 2100 scenario group. While growth mechanisms of otoliths and  
208 their morphogenesis during the early life stages of fish are poorly understood, shifts in otolith shape  
209 are linked to physiological modifications due to environmental disturbance (Geffen, 1987; Vignon,  
210 2018). Early life stages are more vulnerable to environmental challenges because they have higher  
211 surface area to volume ratios and have not yet fully developed the homeostatic regulatory  
212 mechanisms which are found in adult fish (Hurst et al., 2013). For Downs herring, a shift affecting  
213 larval condition has previously been observed *in situ* for individuals at 13 mm, and was driven by  
214 environmental conditions (temperature and prey concentration) (Dennis et al., 2017). Our  
215 experimental study on Downs herring covered this length range but the otoliths did not show any

216 ontogenetic differences. Several previous studies showed that the increase in otolith area by fish size  
217 could mainly result from water acidification (Checkley et al., 2009; Munday et al., 2011; Réveillac et  
218 al., 2015; Coll-Llado et al., 2018). Moreover, the elevated seawater CO<sub>2</sub> can cause directional  
219 asymmetry (Holmberg et al., 2019). For herring, the environmental factors we studied  
220 (temperature/CO<sub>2</sub>) did not affect the otolith shape between sides at the observed larval stage.  
221 Consequently, it is likely that the level of response to CO<sub>2</sub> increase might be a species-specific  
222 phenomenon. This capacity to maintain otolith shape in response to environmental changes is  
223 probably due to efficient intracellular ionic-regulation mechanisms in this species (Ishimatsu et al.,  
224 2008; Melzner et al., 2009). This result may suggest that herring larvae are well equipped to cope  
225 with the environmental changes projected for 2100, as long as their energy and nutritional needs are  
226 well covered, which would not necessarily be the case in the natural environment. The faster growth  
227 of the larvae under the 2100 scenario may indeed lead to a greater prey requirement, and it cannot be  
228 ruled out that the increase in the area of the otoliths may also have affected their hearing ability and  
229 behaviour. Nevertheless, it should be noted that this species certainly has a good intracellular ionic  
230 regulation because it is confronted with different environments (Ishimatsu et al., 2008; Melzner et al.,  
231 2009). Indeed, herring larvae typically hatch in littoral regions where pH and temperature can  
232 fluctuate because of freshwater inflow, so they may often experience such fluctuations and therefore  
233 be quite resistant to them. For more extreme values, however, the homeostatic mechanisms might not  
234 be sufficient to compensate for environmental stress and this could induce changes in otolith  
235 morphological development (Coll-Llado et al., 2018).

236 Ontogeny and environment are the factors that control most of the otolith development during the  
237 early stages of life. The otolith shape evolves from the basic round form to elongated shape due to  
238 faster growth along the anterior-posterior axis than along the dorsal-ventral axis (Galley et al., 2006;  
239 Mille et al., 2015; Bounket et al., 2019; Mahé et al., 2019). Our study showed that the otolith shape

240 of herring grew in this way during the larval period. At the adult stage, significant directional  
241 asymmetry has been observed in herring (Bird et al., 1986), while no lateralization has been observed  
242 at the larval stage. This bilateral effect increases over the life of the fish when considering a different  
243 trajectory of otolith morphogenesis between left and right sides. However, the asymmetry between  
244 left and right otoliths especially the fluctuating asymmetry may be underestimated in experiments  
245 due to the small number of tested individuals which are experiencing stressful conditions and present  
246 experimental conditions that do not require significant development of acoustic functions as in the natural  
247 environment (Grønkjær and Sand, 2003; Diaz-Gil et al., 2015). Consequently, no lateralization has  
248 been observed in the experimental condition for the herring larval stage does not mean that this result  
249 will be the same in the natural environment. Although otolith shape is influenced by both abiotic and  
250 biotic environmental parameters and depends on individuals' genotype, environmental effects can  
251 also be perceived more with ontogeny, consequently, this developmental lateralization could be a  
252 phenotypically plastic response to environmental drivers rather than the consequence of the  
253 individual genotype, as previously suggested in *Boops boops* (Mahé et al., 2018). Sagittal otolith size  
254 and shape for each species could therefore be adaptive traits to different habitats and ecological  
255 niches (Lychakov and Rebane, 2000; Lombarte et al., 2010).

## 256 **Conclusions**

257 The growth and shape of the otoliths studied here did not appear to be affected by the environmental  
258 conditions predicted for 2100. However, this experimental approach should be confirmed *in situ*.  
259 Only the relationship between otolith and fish sizes seems to be environment-dependent. This  
260 information is important to understand the otolith morphogenesis and consequently when the otolith  
261 shape was used as a tool in fisheries science. In the future, to complete this approach, a crossed-effect  
262 experiment (four different settings: control, temperature increase, acidification, temperature increase  
263 and acidification) could be applied to quantify the effect of each environmental factor. In the same

264 way, it could be important to understand the link between the environment modifications and the  
265 food consumption by fish to separate the direct and indirect effects of the climate change on the  
266 otolith and fish growth.

## 267 **5. Acknowledgments**

268 This work was supported by the Institut Français de Recherche et d'Exploitation de la Mer and the  
269 Alfred Wegener Institute (AWI-MARUM-IFREMER partnership program, "CoCkAIL" Climate  
270 ChAnge effect on fIsh Larvae, doctoral support to L. Joly, 2018-2022).

271 The authors thank technicians, researchers and students who helped to carry this experiment, Valérie  
272 Lefebvre, Margaux Denamiel, Antoine Dussuel, Thibaut Kersaudy, Josselin Caboche, Clémence  
273 Couvreur, Pierre Cresson, Christophe Loots, Sophie Collet, Lauriane Madec, David Mazurais, Clara  
274 Ortu, Marie-Madeleine Le Gall and Jean-Baptiste Quéméneur. Logistic aid was also provided by the  
275 Nausicaä Centre National de la Mer and in particular by Stéphane Hénard. Finally, this work would  
276 have not been possible without the involvement of local fishermen (CME, From Nord) in Boulogne-  
277 Sur-Mer willing to support science and research on highly important local fish species. The authors  
278 are grateful to Aquastream Company and to all members of the LEMAR-ARN team of the Ifremer-  
279 Centre de Bretagne, who contributed to this work.

## 280 **4. References**

281 Berg, F., Husebø, A., Aanestad Godiksen, J., Slotte, A., Folkvord, A., 2017. Spawning time of  
282 Atlantic herring (*Clupea harengus*) populations within a restricted area reflects their otolith growth at  
283 the larval stage, *Fish. Res.* 194: 68-75, doi:10.1016/j.fishres.2017.05.009.

284 Bignami, S., Sponaugle, S., Cowen, R., 2013. Response to ocean acidification in larvae of a large  
285 tropical marine fish, *Rachycentron canadum*. *Glob. Chang. Biol.* 19: 996-1006,  
286 doi:10.1111/gcb.12133.

- 287 Bivand, R.S., Pebesma, E., Gomez-Rubio., V., 2013. Applied spatial data analysis with R, Second  
288 edition. New York: Springer.
- 289 Borcard, D., Gillet, F., Legendre., P., 2011. Numerical ecology with R. Springer, New York
- 290 Bounket, B., Gibert, P., Gennotte, V., Argillier, C., Carrel, G., Maire, A., Logez, M., 2019. Otolith  
291 shape analysis and daily increment validation during ontogeny of larval and juvenile European  
292 chub *Squalius cephalus*. *J. Fish. Biol.* 95: 444-452, doi:10.1111/jfb.13976.
- 293 Burke, N., Brophy, D., King, P.A., 2008. Otolith shape analysis: its application for discriminating  
294 between stocks of Irish Sea and Celtic Sea herring (*Clupea harengus*) in the Irish Sea. *ICES J. Mar.*  
295 *Sci.* 65: 1670-1675, doi:10.1093/icesjms/fsn177.
- 296 Carbonara, P., Ciccolella, A., De Franco, F., Palmisano, M., Bellodi, A., Lembo, G., Neglia, C.,  
297 Spedicato, M.T., Zupa, W., Guidetti, P., 2022. Does fish growth respond to fishing restrictions within  
298 Marine Protected Areas? A case study of the striped red mullet in the south-west Adriatic Sea  
299 (central Mediterranean). *Aquatic Conservation: Marine and Freshwater Ecosystems*, 32(3): 417-429,  
300 doi:10.1002/aqc.3776.
- 301 Cardinale, M., Doering-Arjes, P., Kastowsky, M., Mosegaard., H., 2004. Effects of sex, stock, and  
302 environment on the shape of known-age Atlantic cod (*Gadus morhua*) otoliths. *Can. J. Fish. Aquat.*  
303 *Sci.* 61: 158-167, doi:10.1139/f03-151.
- 304 Casselman, J.M., 1987. Determination of age and growth, p. 209-242. In A.H. Weatherley and H.S.  
305 Gill [eds.], *The Biology of Fish Growth*. Academic Press.
- 306 Checkley, D.M., Dickson, A.G., Takahashi, M., Radich, J.A., Eisenkolb, N.R., 2009. Elevated CO<sub>2</sub>  
307 Enhances Otolith Growth in Young Fish. *Science* 324: 1683, doi:10.1126/science.1169806.

- 308 Chezik, K.A., Lester, N.P., Venturelli, P.A., 2014. Fish growth and degree-days I: Selecting a base  
309 temperature for a within-population study. *Can. J. Fish. Aquat. Sci.* 71(1): 47-55, doi:10.1139/cjfas-  
310 2013-0295.
- 311 Coll-Lladó, C., Mittermayer, F., Webb, P.B., Allison, N., Clemmesen, C., Stiasny M., Bridges, C.R.,  
312 Göttler, G., Garcia de la serrana, D., 2021. Pilot study to investigate the effect of long-term exposure  
313 to high pCO<sub>2</sub> on adult cod (*Gadus morhua*) otolith morphology and calcium carbonate deposition.  
314 *Fish Physiol. Biochem.* 47: 1879-1891, doi:10.1007/s10695-021-01016-6.
- 315 Coll-Lladó, C., Giebichenstein, J., Webb, P.B., Bridges, C.R., Garcia de la Serrana, D., 2018. Ocean  
316 acidification promotes otolith growth and calcite deposition in gilthead sea bream (*Sparus aurata*)  
317 larvae. *Sci Rep* 8: 8384, doi:10.1038/s41598-018-26026-y.
- 318 Díaz-Gil, C., Palmer, M., Catalán, I.A., Alós, J., Fuiman, L.A., García, E., del Mar Gil, M., Grau, A.,  
319 Kang, A., Maneja, R.H., Mohan, J.A., Morro, B., Schaffler, J.J., Buttay, L., Riera-Batle, I., Tolosa,  
320 B., Morales-Nin, B., 2015. Otolith fluctuating asymmetry: a misconception of its biological  
321 relevance?, *ICES Journal of Marine Science* 72(7): 2079–2089, doi:10.1093/icesjms/fsv067.
- 322 Degens, E.T., Deuser, W.G., Haedrich, R.L., 1969. Molecular structure and composition of fish  
323 otoliths. *Mar. Biol.* 2: 105-113, doi:10.1007/BF00347005.
- 324 Denis, J., Mahé, K., Tavernier, E., Monchy, S., Vincent, D., Vallet, C., Marchal, P., Antajan, E.,  
325 Caboche, J., Lefebvre, V., Cordier, R., Loots, C., 2017. Ontogenetic changes in the larval condition  
326 of Downs herring: use of a multi-index approach at an individual scale. *Mar Biol* 164: 154,  
327 doi:10.1007/s00227-017-3180-3.

- 328 Enberg, K., Jorgensen, C., Dunlop, E.S., Varpe, O., Boukal, D.S., Baulier, L., Eliassen, S., Heino,  
329 M., 2011. Fishing-induced evolution of growth: concepts, mechanisms and the empirical evidence.  
330 *Mar. Ecol.*, 33:1-25, doi: 10.1111/j.1439-0485.2011.00460.x.
- 331 Folkvord, A., Johannessen, A., Moksness, E., 2004. Temperature-dependent otolith growth in  
332 Norwegian spring-spawning herring (*Clupea harengus* L.) larvae. *Sarsia* 89: 297-310,  
333 doi:10.1080/00364820410002532.
- 334 Folkvord, A., Rukan, K., Johannessen, A., Moksness, E., 1997. Early life history of herring larvae in  
335 contrasting feeding environments determined by otolith microstructure analysis. *J. Fish. Biol.* 51:  
336 250-263, doi:0022-1 112/97/51A250+ 14 \$25.0010.
- 337 Franke, A., Clemmesen, C., 2011. Effect of ocean acidification on early life stages of Atlantic herring  
338 (*Clupea harengus* L.), *Biogeosciences*, 8(12): 3697-3707, doi:10.5194/bg-8-3697-2011.
- 339 Frommel, A.Y., Schubert, A., Piatkowski, U., Clemmesen, C., 2013. Egg and early larval stages of  
340 Baltic cod, *Gadus morhua*, are robust to high levels of ocean acidification. *Mar. Biol.* 160: 1825-  
341 1834, doi:10.1007/s00227-011-1876-3.
- 342 Galley, E.A., Wright, P.J., Gibb, F.M., 2006. Combined methods of otolith shape analysis improve  
343 identification of spawning areas of Atlantic cod. *ICES J. Mar. Sci.* 63 : 1710-1717,  
344 doi:10.1016/j.icesjms.2006.06.014.
- 345 Geffen, A.J., 1987. Methods of validating daily increment deposition in otoliths of larval fish, in *Age*  
346 *and growth of fish*, Summerfelt RC, Hall GE editors. Iowa State University Press, 223–240.
- 347 GrønkJær P., Sand, M.K., 2003. Fluctuating asymmetry and nutritional condition of Baltic cod  
348 (*Gadus morhua*) larvae. *Mar. Biol.* 143: 191-197. doi: 10.1007/s00227-003-1064-1. Holmberg, R.J.,  
349 Wilcox-Freeburg, E., Rhyne, A.L., Tlusty, M.F., Stebbins, A., Nye, Jr.S.W., Honig, A., Johnston,

- 350 A.E., San Antonio, C.M., Bourque, B., Hannigan, R.E., 2019. Ocean acidification alters morphology  
351 of all otolith types in Clark's anemonefish (*Amphiprion larkii*). *PeerJ* 7:e6152, doi:  
352 10.7717/peerj.6152.
- 353 Hönisch, B., Ridgwell, A.J., Schmidt, D.N., Thomas, E., Gibbs, S.J., Sluijs A., Zeebe, R., Kump, L.,  
354 Martindale, R.C., Greene, S.E., Kiessling, W., Ries, J., Zachos, J.C., Royer, D.L., Barker, S.,  
355 Marchitto Jr., T.M., Moyer, R., Pelejero, C., Ziveri, P., Foster, G.L., Williams, B., 2012. The  
356 geological record of ocean acidification. *Science* 335: 1058-1063, doi:10.1126/science.1208277.
- 357 Hufnagl, M., Peck, M.A., 2011. Physiological individual-based modelling of larval Atlantic herring  
358 (*Clupea harengus*) foraging and growth: insights on climate-driven life-history scheduling, *ICES J.*  
359 *Mar. Sci.* 68: 1170-1188, doi:10.1093/icesjms/fsr078.
- 360 Hurst, T., Fernandez, E., Mathis, J., 2013. Effects of ocean acidification on hatch size and larval  
361 growth of walleye pollock (*Theragra chalcogramma*), *ICES J. Mar. Sci.* 70: 812-822,  
362 doi:10.1093/icesjms/fst053.
- 363 Hüsey, K., 2008. Otolith shape in juvenile cod (*Gadus morhua*): Ontogenetic and environmental  
364 effects. *J. Exp. Mar. Bio. Ecol.* 364: 35-41, doi:10.1016/j.jembe.2008.06.026.
- 365 Hüsey, K., Limburg, K.E., de Pontual, H., Thomas, O.L.R., Cook, P.K., Heimbrand Y., Blass, M.,  
366 Sturrock, A.M., 2020. Trace Element Patterns in Otoliths: The Role of Biomineralization, *Rev. Fish.*  
367 *Sci. Aquac.* 29(4): 445-477, doi:10.1080/23308249.2020.1760204.
- 368 IPCC, 2014. Climate change 2014: Synthesis report. Contribution of Working Groups I, II and III to  
369 the fifth assessment report of the Intergovernmental Panel on Climate Change. IPCC 2014,  
370 <http://hdl.handle.net/10013/epic.45156>

371 Irgens, C., 2018. Otolith structure as indicator of key life history events in Atlantic cod (*Gadus*  
372 *morhua*). Ph.D. thesis. Univ. of Bergen.

373 Ishimatsu, A., Hayashi, M., Kikkawa, T., 2008. Fishes in high-CO<sub>2</sub>, acidified oceans, *Mar. Ecol.*  
374 *Prog. Ser.* 373: 295-302, doi:10.3354/meps07823.

375 Johannessen, A., Blom, G., Folkvord, A., 2000. Differences in growth pattern between spring and  
376 autumn spawned herring (*Clupea harengus* L.) larvae. *Sarsia* 85: 461-466,  
377 <http://dx.doi.org/10.1080/00364827.2000.10414595>.

378 Joly, L.J., Loots, C., Meunier, C.L., Boersma, M., Collet, S., Lefebvre, V., Zambonino-Infante, J.L.,  
379 Giraldo, C., 2021. Maturation of the digestive system of Downs herring larvae (*Clupea harengus*,  
380 Linnaeus, 1758): identification of critical periods through ontogeny. *Mar. Biol.* 168: 82,  
381 doi:10.1007/s00227-021-03894-z.

382 Kuhl, F., Giardina, C., 1982. Elliptic Fourier features of a closed contour. *Comput. Graph. Image*  
383 *Proc.* 18: 236-258, doi:10.1016/0146-664X(82)90.

384 Legendre, P., Legendre, L.F.J., 1998. *Numerical Ecology*. Elsevier Science.

385 Lestrel, P.E., 2008. *Fourier Descriptors and their Applications in Biology*. Cambridge University  
386 Press.

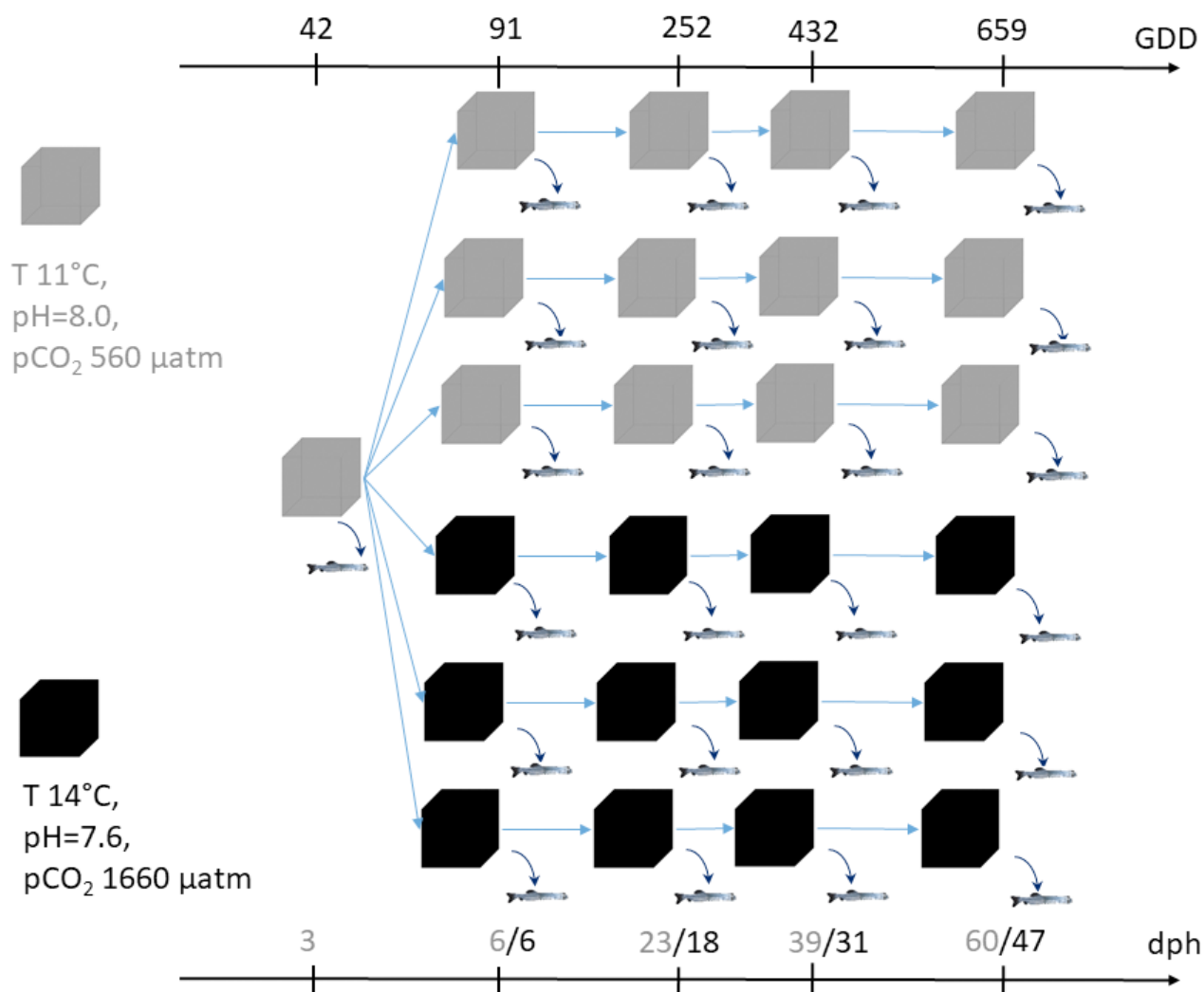
387 Libungan, L.A., Óskarsson, G.J., Slotte, A., Jacobsen, J.A., Pálsson, S., 2015. Otolith shape: a  
388 population marker for Atlantic herring *Clupea harengus*. *J. Fish Biol.* 86: 1377-  
389 1395, doi:10.1111/jfb.12647.

- 390 Lombarte, A., Palmer, M., Matallanas, J., Gómez-Zurita, J., Morales-Nin, B., 2010.  
391 Ecomorphological trends and phylogenetic inertia of otolith sagittae in Nototheniidae. *Environ. Biol.*  
392 *Fishes* 89: 607-618, doi:10.1007/s10641-010-9673-2.
- 393 Lychakov, D.V., Rebane, Y.T., 2000. Otolith regularities. *Hear. Res.* 143: 83-102,  
394 doi:10.1016/s0378-5955(00)00026-5.
- 395 Mahé, K., 2019. Sources de variation de la forme des otolithes : implications pour la discrimination  
396 des stocks de poissons. Ph.D. thesis. Univ. of Littoral Côte d'Opale
- 397 Mahé, K., Gourtay, C., Bled Defruit, G., Chantre, C., de Pontual, H., Amara, R., Claireaux, G.,  
398 Audet, C., Zambonino-Infante, J.L., Ernande, B., 2019. Do environmental conditions (temperature  
399 and food composition) affect otolith shape during fish early-juvenile phase? An experimental  
400 approach applied to European Seabass (*Dicentrarchus labrax*). *J. Exp. Mar. Bio. Ecol.* 521: 151239,  
401 doi:10.1016/j.jembe.2019.151239.
- 402 Mahé, K., Ider, D., Massaro, A., Hamed, O., Jurado-Ruzafa, A., Gonçalves, P., Anastasopoulou, A.,  
403 Jadaud, A., Mytilineou, C., Elleboode, R., Ramdane, Z., Bacha, M., Amara, R., de Pontual, H.,  
404 Ernande, B., 2018. Directional bilateral asymmetry in otolith morphology may affect fish stock  
405 discrimination based on otolith shape analysis. *ICES J. Mar. Sci.* 76(1): 232-243,  
406 doi:10.1093/icesjms/fsy163. Maneja, R.H., Frommel, A.Y., Geffen, A.J., Folkvord, A., Piatkowski,  
407 U., Chang M.Y., Clemmesen, C., 2013. Effects of ocean acidification on the calcification of otoliths  
408 of larval Atlantic cod *Gadus morhua*. *Mar. Ecol. Prog. Ser.* 477: 251-258, doi: 10.3354/meps10146.
- 409 Marty, L., Rochet, M.-J., Ernande, B., 2014. Temporal trends in age and size at maturation of four  
410 North Sea gadid species: cod, haddock, whiting and Norway pout. *Mar. Ecol. Prog. Ser.* 497: 179-  
411 197. doi: 10.3354/meps10580

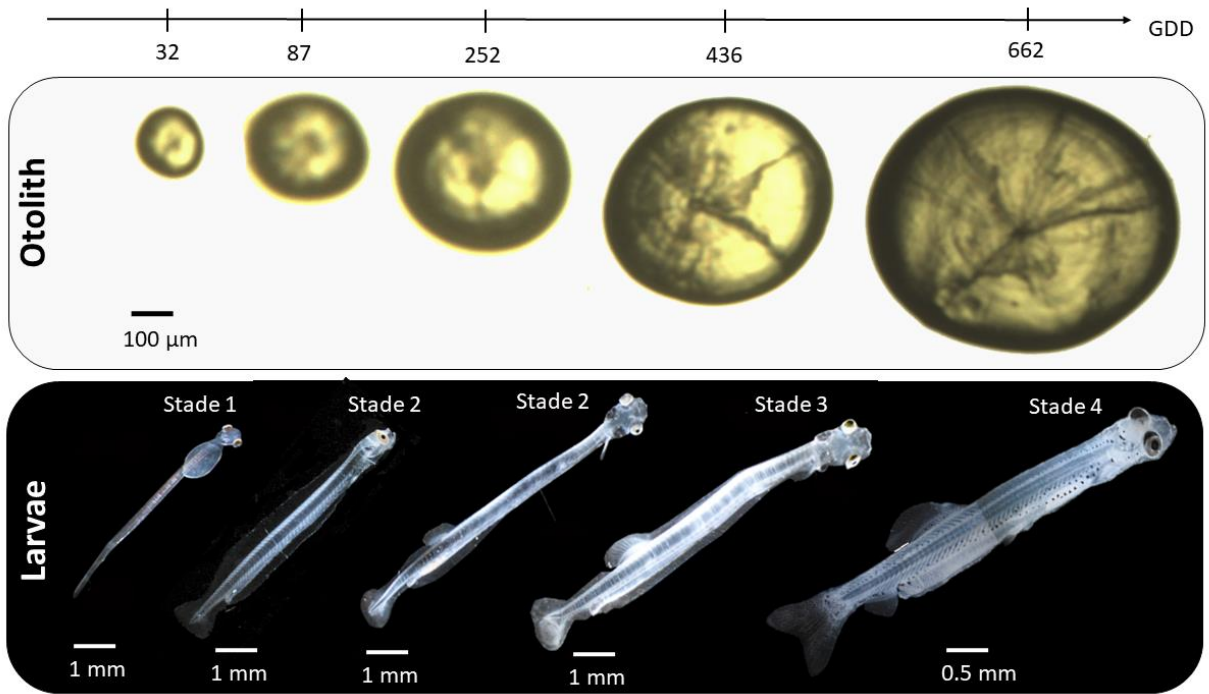
- 412 McMaster, G.S., Wilhelm, W., 1997. Growing degree-days: one equation, two interpretations. *Agric.*  
413 *For. Meteorol.* 87; 291-300. doi:10.1016/S0168-1923(97)00027-0.
- 414 Melzner, F., Gutowska, M.A., Langenbuch, M., Dupont, S., Lucassen, M., Thorndyke, M.C., Bleich,  
415 M., Pörtner, H.O., 2009. Physiological basis for high CO<sub>2</sub> tolerance in marine ectothermic animals:  
416 pre-adaptation through lifestyle and ontogeny?, *Biogeosciences* 6: 2313-2331.  
417 <http://www.biogeosciences.net/6/2313/2009/>.
- 418 Mille, T., Mahé, K., Villanueva, C.M., de Pontual, H., Ernande, B., 2015. Sagittal otolith  
419 morphogenesis asymmetry in marine fishes. *J. Fish Biol.* 87: 646-663, doi:10.1111/jfb.12746.
- 420 Munday, P.L., Gagliano, M., Donelson, J.M., Dixon, D.L., Thorrold, S.R., 2011. Ocean acidification  
421 does not affect the early life history development of a tropical marine fish. *Mar. Ecol. Prog. Ser.* 423:  
422 211-221, doi: 10.3354/meps08990.
- 423 Payan, P., Borelli, G., Boeuf, G., Mayer-Gostan, N., 1998. Relationship between otolith and somatic  
424 growth: consequence of starvation on acid-base balance in plasma and endolymph in the rainbow  
425 trout *Oncorhynchus mykiss*. *Fish Phys. Bioch.* 19: 35-41, doi:10.1023/A:1016064813517.
- 426 Perry, D.M., Redman, D.H., Widman Jr, J.C., Meseck, S., King, A., Pereira, J.J., 2021. Effect of  
427 ocean acidification on growth and otolith condition of juvenile scup, *Stenotomus chrysops*. *Ecol.*  
428 *Evol.* 5(18): 4187-4196, doi:10.1002/ece3.1678.
- 429 Popper, A.N., Ramcharitar, J., Campana, S.E., 2005. Why otoliths? Insights from inner ear  
430 physiology and fisheries biology. *Mar. Freshw. Res.* 56 : 497-504,  
431 <https://dx.doi.org/10.1071/mf04267>

- 432 Réveillac, E., Lacoue-Labarthe, T., Oberhänsli, F., Teyssié, J.L., Jeffree, R., Gattuso, J.P., Martin, S.,  
433 2015. Ocean acidification reshapes the otolith-body allometry of growth in juvenile sea bream. *J.*  
434 *Exp. Mar. Bio. Ecol.* 463: 87-94, doi:10.1016/j.jembe.2014.11.007.
- 435 Rohlf, F.J., Archie, J.W., 1984. A Comparison of Fourier Methods for the Description of Wing Shape  
436 in Mosquitoes (Diptera: Culicidae). *Syst. Biol.* 33: 302-317, doi:10.2307/2413076.
- 437 Tonheim, S., Slotte, A., Andersson, L., Folkvord A., Berg, F., 2020. Comparison of Otolith  
438 Microstructure of Herring Larvae and Sibling Adults Reared Under Identical Early Life  
439 Conditions. *Front. Mar. Sci.* 7: 529, doi:10.3389/fmars.2020.00529.
- 440 Turan, C., 2000. Otolith shape and meristic analysis of herring (*Clupea harengus*) in the North-East  
441 Atlantic. *Arch. Fish. Mar. Res.* 48: 283-295.
- 442 Vignon M., 2018. Short-term stress for long-lasting otolith morphology – Brief embryological stress  
443 disturbance can reorient otolith ontogenetic trajectory. *Can. J. Fish. Aquat. Sci.* 75(10): 1713-1722,  
444 doi:10.1139/cjfas-2017-0110.
- 445 Vignon, M., Morat, F., 2010. Environmental and genetic determinant of otolith shape revealed by a  
446 non-indigenous tropical fish. *Mar. Ecol. Prog. Ser.* 411: 231-241, doi:10.3354/meps08651.
- 447
- 448
- 449
- 450
- 451

452 Figure 1: Main steps of the experimental design for herring with five samplings by the level of GDD  
 453 (Growing Degree Days) and by the number of dph (Days Post Hatching; grey value for 11°C; black  
 454 value for 14°C). Each condition of temperature and CO<sub>2</sub> concentration had three replicates. To test  
 455 the effect of global change, present day conditions (11°C and pH 8.0, pCO<sub>2</sub> 560 μatm) versus the  
 456 ocean warming and acidification conditions predicted for 2100 (14°C and pH 7.6, pCO<sub>2</sub> 1660 μatm)  
 457 were used.



461 Figure 2: Growth of otolith shape and larval fish by GDD value (°C.day).



462

463

464

465

466

467

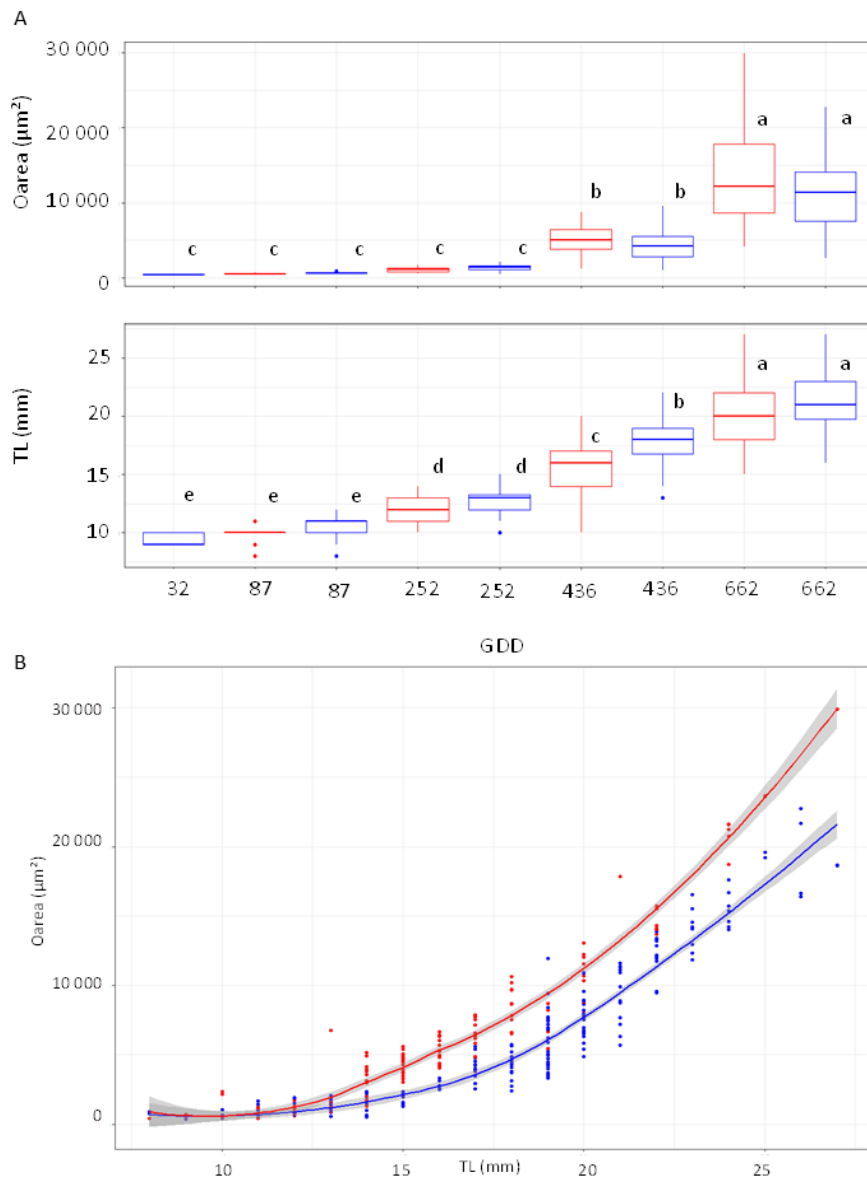
468

469

470

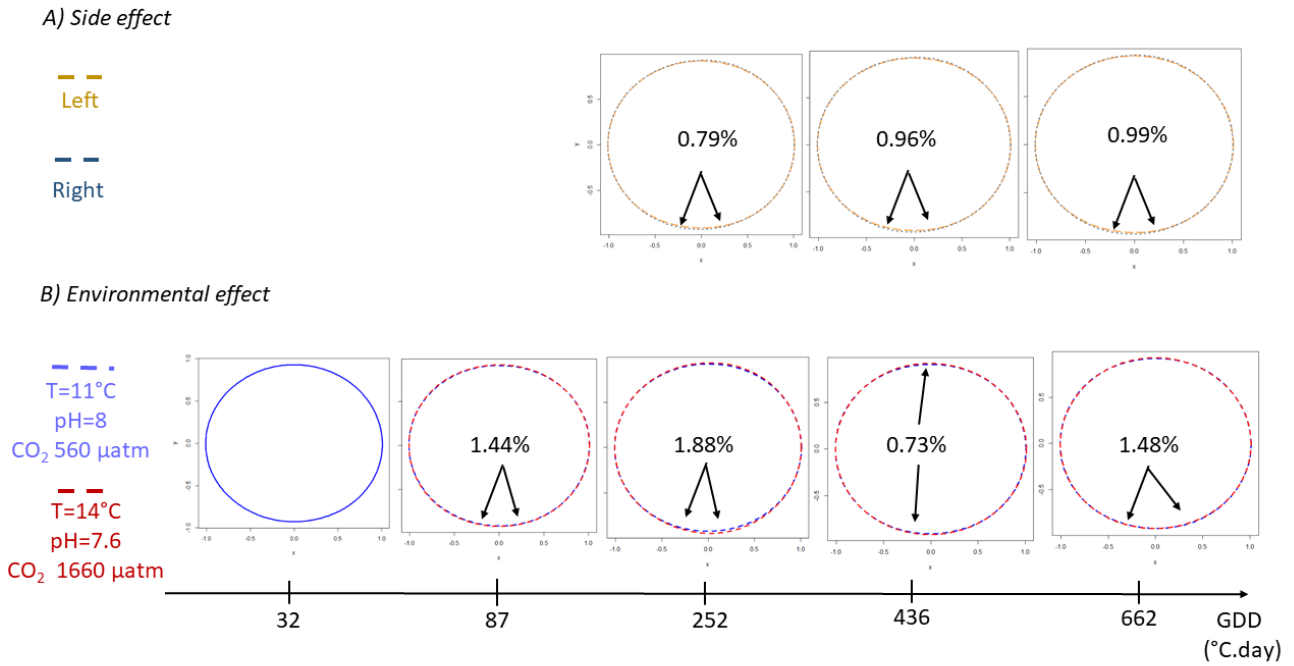
471

472 Figure 3: (A) Box-plot of otolith area (Oarea,  $\mu\text{m}^2$ ) and total length of fish (TL, cm) values by GDD  
 473 value ( $^{\circ}\text{C}\cdot\text{day}$ ) and environmental conditions (red for  $14^{\circ}\text{C}$  and  $1660 \mu\text{atm}$ , and blue for  $11^{\circ}\text{C}$  and  
 474  $560 \mu\text{atm}$ ). A different letter within each sampling time denotes a significant difference between the  
 475 two groups. (B) Relationship between otolith average area (Oarea) and larval body length (TL) in  
 476 response to the environmental conditions (red for  $14^{\circ}\text{C}$  and  $1700 \mu\text{atm}$ , and blue for  $11^{\circ}\text{C}$  and  $560$   
 477  $\mu\text{atm}$ ) (smoothing method using level of confidence interval of 0.95).



478

479 Figure 4: Percentage of non-overlapping surface between left and right otolith shape and for two  
 480 environmental conditions by GDD value ( $^{\circ}\text{C}\cdot\text{day}$ ) (arrows identify the main areas of difference  
 481 between both otoliths).



482

483

484

485

486

487

488

489

490 **Effect of climate change on the morphogenesis of sagittal otoliths in**  
 491 **Atlantic herring (*Clupea harengus*) larvae**

*Supplementary Material*

492 **Kélig Mahé<sup>1\*</sup>, Léa Justine Joly<sup>1,2</sup>, Solène Telliez<sup>1</sup>, José Luis Zambonino-Infante<sup>2</sup>, Cédric Léo**  
 493 **Meunier<sup>3</sup>, Kirsteen M. MacKenzie<sup>1</sup>, Carolina Giraldo<sup>1</sup>**

494 <sup>1</sup>Ifremer, Fisheries laboratory, Channel and North Sea Fisheries Research Unit, Boulogne-sur-mer,  
 495 France

496 <sup>2</sup> Ifremer, Univ Brest, CNRS, IRD, LEMAR, F-29280 Plouzané, France

497 <sup>3</sup>Helmholtz-Zentrum für Polar- und Meeresforschung, Alfred-Wegener-Institut, Helgoland, Germany

498

***Supplementary Table S1. Water parameters (Mean  $\pm$  sd) during the larval rearing of herring larvae from 32 to ~670°C.day***

Condition	T (°C)	pH	S (psu)	TA ( $\mu\text{mol/kgSW}$ )	pCO <sub>2</sub> ( $\mu\text{atm}$ )
Amb (11°C, 650 $\mu\text{atm}$ ) n= 6	11.3 $\pm$ 0.4	8.03 $\pm$ 0.04	32.7 $\pm$ 0.4	2275.2 $\pm$ 139.3	559.1 $\pm$ 55.9
OWA (14°C, 1660 $\mu\text{atm}$ ) n = 6	14.2 $\pm$ 0.5	7.61 $\pm$ 0.12	32.7 $\pm$ 0.4	2280.3 $\pm$ 150.4	1661.6 $\pm$ 291.3

***Supplementary Table S2: Summary of redundancy analyses of herring otolith shapes.***

Factor	df	P-value
Side	1	0.756
T°C/pCO <sub>2</sub>	1	0.097
GDD	8	0.118

499

500